

Three-dimensional Radar Imaging Based on Sparse Measurements

Zou Xin, Zhou Jianxiong and Fu Qiang

Laboratory ATR, School of Electronic Science and Engineering, National University of Defense Technology,
Changsha, China

Email: zouhaijun2@163.com

Abstract. In conventional three-dimensional Inverse Synthetic Aperture Radar (ISAR) imaging, high range-resolution is attained by transmitting a wideband signal and high cross-range resolution is attained by increasing the observation azimuth and elevation. Consequently, large collection time and data storage is needed for this three-dimensional imaging method. This paper presents three-dimensional imaging approaches by using the sparse measurements and convex optimization. This approach could decrease data collection time and data storage amount greatly; the proposed approaches have been verified using numerical simulations of point target, which show that it could recover the image exactly and maintain the imaging resolution.

Keywords: 3D ISAR; Sparse measurement; Compressed sensing; Three-dimensional imaging

1. Introduction

The three-dimensional (3-D) imaging of radar targets has been widely used for target identification, target scattering modeling, as well as studies of target scattering mechanisms [1] [2]. Such images provide robust target characterization and feature identification of specific scatters on any given target.

Conventional three-dimensional (3-D) ISAR imaging requires a collection of radar returns from a densely sampled set of points in both azimuth and elevation angle over a scene. Image resolution is improved by increasing the extent of these passes in azimuth and elevation. Hence, high resolution imagery requires large data collection time and storage capacity [3], which is hard to achieve in reality [4].

We could also obtain the 3-D imagery by the Fourier Transform of the sparse 3D data from the sampling of the full aperture data, but the reconstructed image will be smoothed and contain artifacts, that is, the reconstruction quality is poor. The Compressed Sensing (CS) theory has showed that a super-resolved signal and images can be reconstructed from far fewer data than what is needed by the Nyquist/Shannon sampling theory [5][6]. For high-resolution images at high frequencies, the scattering response of an object can be well approximated as a sum of responses from individual reflectors [7], and thus are compressible; this made us use the sparse measurements and sparse reconstruction algorithm to recover the 3D image of the target. Meanwhile, we hope the resolution of the image can be maintained.

In this work, we present a three-dimensional imaging algorithm which is based on Compressed Sensing and sparse measurement. This paper is organized as follows. In Section II, we present the geometry model between radar and target and sparse ISAR data collection. Section III discusses an algorithm for a 3D image reconstruction for sparse measurement. Finally, in Section IV, we present a 3D image reconstruction example using point target simulation data. This example demonstrates that it is possible to form accurate 3D ISAR images with well-resolved features from sparse data collected.

2. The Geometry Model and Sparse Isar Data Collection

2.1. The Geometry Model

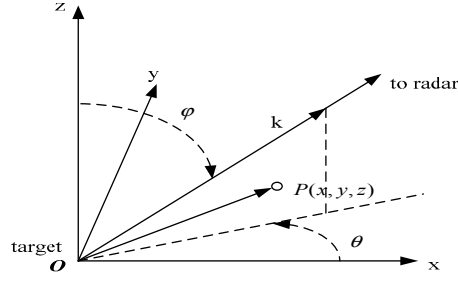


Fig.1. Geometry model between radar and target

The geometry model between the radar and target is illustrated in Fig.1; the origin of the coordinate system (x, y, z) is the center of the target and fixed on it, k is the direction of the radar to the scene center, O is the scene center, and P is the scatter location. We assume that the radar transmits a stepped-frequency signal with bandwidth B centered about a center frequency f_c . We also assume that the transmitter is sufficiently far away from the scene so that wavefront curvature is negligible, and we use a plane wave model for reconstruction [3]. θ is the azimuth sensor position, and φ is the sensor position in elevation. After mixing the return signal with the transmitted signal, delayed by the time to scene center, demodulating, and neglecting a quadratic phase term, the final received signal is [6]:

$$r(t) = \int_{-B_z}^{B_z} \int_{-B_y}^{B_y} \int_{-B_x}^{B_x} \alpha(x, y, z; \theta, \varphi, f, pol) \times e^{-jK(t)k} dx dy dz \quad (1)$$

Where f is the frequency of the radar signal, pol is the polarization of the radar signal, the scene reflectivity function is given by $\alpha(x, y, z; \theta, \varphi, f, pol)$, boundaries of the scene in each dimension are $B_{(i)}$. $K(t)$ is a linear function of time and is supported on $\frac{4\pi}{c}[f_c - \frac{B}{2}, f_c + \frac{B}{2}]$, where c is the speed of light. By the projection-slice theorem, it follows that the Fourier transform of the scene reflectivity function projected onto the direction k is equivalent to a line along the k in 3D k -space of the scene reflectivity function. The three-dimensional Fourier Transform of α is given by:

$$G = \int \alpha(x, y, z; \theta, \varphi, pol) e^{-j(k_x x + k_y y + k_z z)} dx dy dz \quad (2)$$

where

$$k_x = \frac{4\pi f}{c} \cos \theta \sin \varphi, k_y = \frac{4\pi f}{c} \sin \theta \sin \varphi, k_z = \frac{4\pi f}{c} \cos \varphi \quad (3)$$

For narrow-angle measurements, it is often assumed that the scene reflectivity is isotropic; so, α is not a function of (θ, φ) . Using the GDT model, the returned signal from an object to be imaged can be represented as the integration of the contributions from all scatters in the object:

$$E(X, Y, Z) = \sum_{k=1}^K \alpha_k(x, y, z; \theta, \varphi, f, pol) e^{-j(k_x x + k_y y + k_z z)} \quad (4)$$

where $\alpha_k(x, y, z; \theta, \varphi, f, pol)$ is the reflectivity function of a point scatterer at (x, y, z) .

2.2. Sparse Data Collection

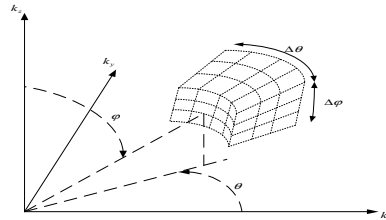


Fig.2. Geometry in the spatial frequency domain and the raw data

Sparse measurements are those obtained by reducing the measurement angle of azimuth and elevation compared to full aperture measurement. We assume that the azimuth is supported on $(\theta_1 : d\theta : \theta_N)$, elevation $(\varphi_1 : d\varphi : \varphi_p)$ and the frequency of the radar signal $(f_1 : df : f_M)$, the data we collect is on the non-uniform k -space grid, as in Fig. 2, thus the look-angle of the observation is $N \times P$. If we just use n azimuth and p elevation,

then, the data will be $\frac{n \times p}{N \times P}$ as the full aperture data. When n and p is small compared to N and P , the saved data will be great. In general, we randomize the look-angle as the left panel in figure 3. Another observation mode is Curve Aperture; see the right panel of Fig. 3.

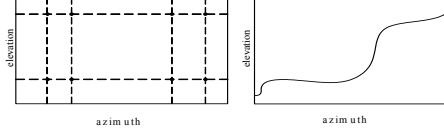


Fig.3. Two mode of sparse measurement

3. Sparse 3D Imaging Reconstruction Algorithms

In section II, two mode of sparse measurement were discussed. When the received data is sparse, how to recover the 3-D image is concerned. In this section, we will present a 3-D imaging algorithm. The proposed approach assumes that the number of 3D locations in which nonzero backscattering occurs is sparse in the 3-D reconstruction space and the complex magnitude response of each scattering center is approximately constant over narrow aspect angles and across the radar frequency bandwidth.

The 3-D image reconstruction is equal to the scatter coefficients estimation of the scene. First, divide the scene into a uniform 3-D grid; assume that the imaging resolution is Δ_x , Δ_y , Δ_z ,

$$\Delta_x = \frac{c}{2B}, \Delta_y = \frac{c}{2f_c \Delta\theta}, \Delta_z = \frac{c}{2f_c \Delta\varphi} \quad (5)$$

where c is the speed of light, B and f_c is the bandwidth and center frequency of the transmitting signal, $\Delta\theta$ and $\Delta\varphi$ is the bounds of the azimuth and elevation. As in section II, the transmitting signal is a stepped-frequency signal and the number of the frequency is M . Also, the number of the azimuth and elevation is N and P , thus the size of the scene could be covered is $(M\Delta_x, N\Delta_y, P\Delta_z)$, and is divided into a uniform 3-D grid with the size $M \times N \times P$, we only need find the scatter coefficient over every grid, then the 3-D image of the scene is recovered. Define C is all locations in image reconstruction space as candidate scattering center locations, $C = \{(x_i, y_i, z_i) | i = 1, \dots, L\}$, where $L = M \times N \times P$, the scatter coefficient of each location is $\alpha_i, i = 1, \dots, L$.

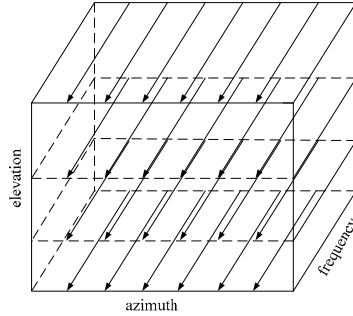


Fig.4. Sparse measurement and candidate scatterer coefficients are ranked

Sparse measurement is the sampling of the full aperture collection. Suppose that the sequence of look-angle is $\{(\theta_i, \varphi_j) | i = 1, \dots, n, j = 1, \dots, p\}$, with n and p just as in section II. Here, the n azimuths and p elevations are selected from the N azimuths and P elevations of full aperture randomly. Assume that the sparse measurement is \mathbf{E}_s with the size $M \times n \times p$. Range this matrix down rows as Fig. 4, then we get the measurements vector \mathbf{y} with the size $M \cdot n \cdot p \times 1$. Define partitioned matrix $\mathbf{A} = [\mathbf{A}_1 \ \mathbf{A}_2 \ \dots \ \mathbf{A}_{n \cdot p}]^T$, every partial matrix $\mathbf{A}_i, i = 1, \dots, n \cdot p$ is the same size as $M \times N \cdot P$.

$$\mathbf{A}_i = \begin{bmatrix} e^{-j f_1 (k_{x1} x_1 + k_{y1} y_1 + k_{z1} z_1)} & \dots & e^{-j f_1 (k_{xN \cdot P} x_{N \cdot P} + k_{yN \cdot P} y_{N \cdot P} + k_{zN \cdot P} z_{N \cdot P})} \\ e^{-j f_2 (k_{x1} x_1 + k_{y1} y_1 + k_{z1} z_1)} & \dots & e^{-j f_2 (k_{xN \cdot P} x_{N \cdot P} + k_{yN \cdot P} y_{N \cdot P} + k_{zN \cdot P} z_{N \cdot P})} \\ \vdots & \dots & \vdots \\ e^{-j f_M (k_{x1} x_1 + k_{y1} y_1 + k_{z1} z_1)} & \dots & e^{-j f_M (k_{xN \cdot P} x_{N \cdot P} + k_{yN \cdot P} y_{N \cdot P} + k_{zN \cdot P} z_{N \cdot P})} \end{bmatrix} \quad (6)$$

where

$$k_{x_i} = \frac{4\pi}{c} \cos \theta_i \sin \varphi_i, k_{y_i} = \frac{4\pi}{c} \sin \theta_i \sin \varphi_i, k_{z_i} = \frac{4\pi}{c} \cos \varphi_i \quad (7)$$

Thus, the measured data from the scattering center model (4) can be written in matrix-vector form as

$$\mathbf{y} = \mathbf{A}\mathbf{x} + \mathbf{n} \quad (8)$$

where $\mathbf{x} = [\alpha_1 \ \alpha_2 \ \cdots \ \alpha_{N,P}]^T$ is the scatter coefficients vector to be reconstructed, and ranged as Fig. 4, \mathbf{n} is the noise vector with the same size as \mathbf{y} .

The number of scattering centers is small compared to the number of reconstructed image voxels in \mathbf{x} , so, \mathbf{x} is sparse. We could recover by the solution of the sparse optimization problem [8]

$$\hat{\mathbf{x}} = \min \|\mathbf{y} - \mathbf{A}\mathbf{x}\|_2^2 + \lambda \|\mathbf{x}\|_1 \quad (9)$$

Here, we use ℓ_1 -norm to constraint the sparsity of the signal, and ℓ_2 -norm to constraint the noise. Many methods have been presented to solve (9), and we will use SPGL1 algorithm [9].

4. Simulation Results

4.1. Point Target Simulation

Table 1. The Coordinate of The Three Point Targets

No.	X	Y	Z	Scatter Intensity
1	-1	-1	-1	1
2	1	1	1	1
3	0	0	0	1

The sparse measurement we used is simulated by three point targets, whose really position and scatter intensity is in Table I. Choosing the observation of center azimuth and elevation are 90° and 90° , the size of azimuth and elevation aperture are 2.86° , the measurement data is collected at every 0.1° azimuth and elevation angle, the transmitted signal is stepped-frequency, with center frequency $10GHz$, stepp length $20MHz$. Thus, the size of the full aperture collected data is $26 \times 29 \times 29$, image resolution is $0.3 \times 0.3 \times 0.3$ meters according to (5), the extent of the image is $(7.8, 8.7, 8.7)$ meters. Select 10 azimuths and 10 elevations data randomly to from the full aperture data, the size of the sparse measurement is $26 \times 6 \times 6$, consists of approximately 11.9% of the full aperture data. Recover the scatter coefficient by SPGL1, and threshold the solution using 0.13, we get the reconstructed scatter coefficient vector, see the left of Fig. 5 and the 3-D image in the right of Fig. 5.

Next, we increase the image resolution to $0.15 \times 0.15 \times 0.15$ meters. Here, the size of azimuth and elevation aperture are 5.7° and the full aperture collected data is $51 \times 58 \times 58$, extend of the image is $(7.8, 8.7, 8.7)$ meters. Select 4 azimuths and 4 elevations data randomly from the full aperture data, the size of this sparse measurement is $51 \times 4 \times 4$, consists of approximately 0.5% of the full aperture data. Recover the scatter coefficient by SPGL1, and threshold the solution using 0.13, we get the reconstructed scatter coefficient vector, see the left of Fig. 6 and the 3-D image in the right of Fig. 6.

4.2. Experiment Analysis

From the results of the simulation in section IV, we can find that, the recovered scattering center is a scatter point of big scattering intensity with some scatter points of small scattering intensity. It has been showed the 3-D imaging algorithm we presented could recover the right coordinate of the point target, demonstrating the validity of our method. A higher resolution and more measurements mean better quality of the reconstruction image. Some artificial scatterers may exist when few measurement is collected, but, the problem is that when the measurement is excessive, the size of the measurement matrix is very large, so we need more time to reconstruct the image.

5. Conclusion

In this paper, we presented a sparse imaging algorithm which connected Compressed Sensing with 3-D ISAR imaging. The sparse measurement collected from random look-angle over the scene, and the 3-D image of the scene is recovered by the SPGL1 algorithm. Data collection time and storage burden are greatly

reduced. In addition, an image reconstruction example using point targets simulation data from a sparse random look-angle was presented. This example demonstrated the validity of our algorithm. In the future, we will study the influence of different sparse measurements and sparse reconstruction algorithms to the image reconstruction.

6. References

- [1] Xu X J, Narayanan R M, Three-dimensional interferometric ISAR imaging for target scattering diagnosis and modeling, IEEE Transactions on Imaging Processing, Vol.10, No.7, pp 1094-1102, Jul.2001
- [2] Zhang Chi, Zhang Xiaoling, Zhang Wei, Research on the Three-dimensional ISAR Imaging for Spin Target, 2007.
- [3] Christian D. Austin, Emre Ertin, and Randolph L. Moses, Sparse Signal Methods for 3D Radar Imaging, Proceedings of the IEEE, 2010. in press.
- [4] Timo Kempf, Markus Peichl, Stephan Dill, Helmut Sues, 3D Tower-Turntable ISAR Imaging, Proceedings of the 4th European Radar Conference, October 2007.
- [5] SHI Guangming, LIU Danhua, GAO Dahua, LIU Zhe, LIN Jie, WANG Liangjun, Advances in Theory and Application of Compressed Sensing, ACTA ELECTRONICA SINICA, Vol.37 No.5, May 2009.
- [6] C.V. Jakowatz, Jr., D.E. Wahl, P.H. Eichel, D.C. Ghiglia, and P.A. Thompson, Spotlight-Mode Synthetic Aperture Radar: A Signal Processing Approach. Boston: Kluwer Academic Publishers, 1996.
- [7] Lee C. Potter, Jason T. Parker, Sparsity and Compressed Sensing in Radar Imaging, Proceedings of the IEEE, Vol. 0, No. 0, 2010. in press.
- [8] M A T Figueiredo, R D Nowak, S J Wright. Gradient projection for sparse reconstruction: Application to compressed sensing and other inverse problems. Journal of Selected Topics in Signal Processing: Special Issue on Convex Optimization Methods for Signal Processing, 2007, 1(4): 586-598.
- [9] Stephen Becker, Jerome Bobin and Emmanuel, J. Candes. NESTA: A Fast And Accurate First-Order method for Sparse Recovery. Applied and Computational Mathematics, Caltech, Pasadena, CA 91125. April 2009.

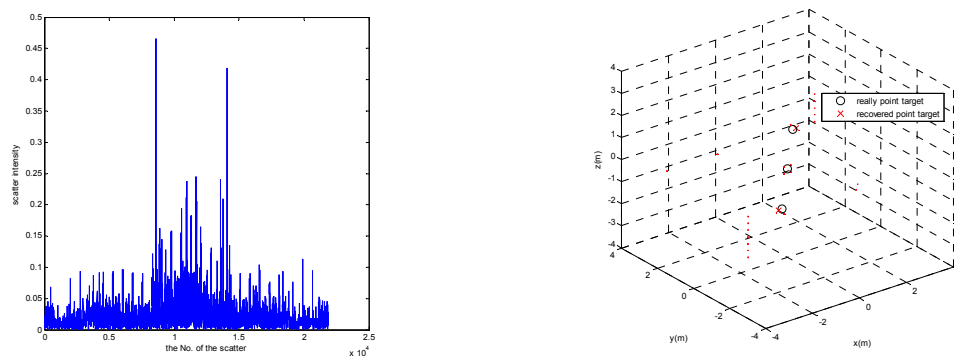


Fig.5. Recovered scatterer coefficient and 3-D image in low image resolution

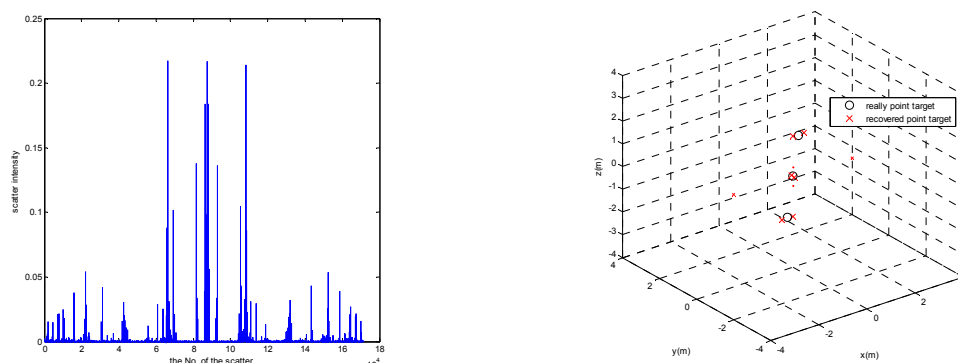


Fig.6. Recovered scatterer coefficient and 3-D image in high image resolution